



The SARS-CoV-2 Y453F mink variant displays a pronounced increase in ACE-2 affinity but does not challenge antibody neutralization

Received for publication, January 28, 2021, and in revised form, March 2, 2021. Published, Papers in Press, March 11, 2021, <https://doi.org/10.1016/j.jbc.2021.100536>

Rafael Bayarri-Olmos¹, Anne Rosbjerg^{1,2}, Laust Bruun Johnsen³, Charlotte Helgstrand³, Theresa Bak-Thomsen³, Peter Garred¹, and Mikkel-Ole Skjoedt^{1,2,*}

From the ¹Laboratory of Molecular Medicine, Department of Clinical Immunology, University Hospital of Copenhagen, Copenhagen, Denmark; ²Institute of Immunology and Microbiology, University of Copenhagen, Copenhagen, Denmark; and ³Novo Nordisk A/S, Måløv, Denmark

Edited by Craig Cameron

Transmission of Severe Acute Respiratory Syndrome Coronavirus 2 from humans to animals has been reported for many domesticated species, including farmed minks. The identification of novel spike gene mutations appearing in minks has raised major concerns about potential immune evasion and challenges for the global vaccine strategy. One genetic variant, known as “cluster five,” arose among farmed minks in Denmark and resulted in a complete shutdown of the world’s largest mink production. However, the functional properties of this new variant are not established. Here we present functional data on the cluster-five variant, which contains a mutation resulting in a Y453F residue change in the receptor-binding domain (RBD) of the spike protein. Using an ELISA-based angiotensin-converting enzyme-2/RBD inhibition assay, we show that the Y453F variant does not decrease established humoral immunity from previously infected individuals or affect the neutralizing antibody response in a vaccine mouse model based on the original Wuhan strain RBD or spike as antigens. However, biolayer interferometry analysis demonstrates that it binds the human angiotensin-converting enzyme-2 receptor with a 4-fold higher affinity than the original strain, suggesting an enhanced transmission capacity and a possible challenge for viral control. These results also indicate that the rise in the frequency of the cluster-five variant in mink farms might be a result of the fitness advantage conferred by the receptor adaptation rather than evading immune responses.

Experimental infection models have shown that Severe Acute Respiratory Syndrome Coronavirus 2 (SARS-CoV-2) is capable of infecting a wide range of animal species, such as cats, dogs, ferrets, and hamsters (1–3), and natural reverse-zoonotic transmission to animals has been documented in farmed mink (4), dogs (5, 6), and felines (6–8). Several variants affecting the spike protein have been documented since the early reports in the spring of 2020 of SARS-CoV-2 transmission from humans to minks (4, 9, 10). The spike protein mediates the binding of SARS-CoV-2 to the human angiotensin-converting enzyme-2 (ACE-2) receptor (11, 12)

and strongly influences the viral infectivity and transmissibility. Moreover, the spike protein is the main target for the host’s protective antibody response (11, 13, 14). Mutations arising through antigenic drift may thus result in novel viral escape strains. One of these cluster variants, disclosed as “cluster five,” has been discovered in Denmark and bears a tyrosine to phenylalanine substitution (Y453F) in the receptor-binding domain (RBD) of the spike protein (15). This position is conserved between SARS-CoV-1 and SARS-CoV-2, and analyses of the crystal structure of SARS-CoV-2 RBD in complex with ACE-2 reveal that it is directly involved in the interaction of the virus with the host cell receptor (16, 17). However, the role of this variant concerning functional transmission and establishment of immunity is unknown. At present, two new RBD variants known as N439K and N501Y have been found in humans. The latter appears to have a better transmission or improved immune evasion than the original counterpart, and this variant is currently increasing in the infection cases in the United Kingdom (18).

There is a general lack of evidence characterizing the pathogenesis, functional properties, and impact on these new cluster variants’ immune recognition and memory responses. Despite this, there have been speculations and reports suggesting that the cluster-five variant might have evasion potential by reducing the immunity of convalescent individuals and that it could even challenge the current global vaccine strategies (15). Based on these presumptions, the Danish government in November 2020 decided to completely shut down all Danish mink farms, which at that time represented the largest mink fur production in the world.

To address the biophysical characteristics and the impact of this variant on established immunity, we expressed recombinant SARS-CoV-2 RBD WT (WT, from the Wuhan-Hu-1/2019 isolate) and “cluster-five” Y453F and the ACE-2 ectodomain. The Y453F variant did not alter the inhibition potency of sera from convalescent individuals exposed to the WT strain in the spring of 2020, nor did it challenge the humoral vaccine response in a mouse model immunized with WT RBD or prefusion-stabilized spike protein ectodomain. However, we found a 4-fold affinity increase of the Y453F variant to the ACE-2 binding that could result in an enhanced spreading potential.

* For correspondence: Mikkel-Ole Skjoedt, moskjoedt@sund.ku.dk.

Results

Biophysical characterization

To determine the biological significance of the Y453F mutation, we studied the impact on protein stability and function by thermal denaturation and binding kinetics experiments (Fig. 1). Using the ratio of the intrinsic fluorescence at 350 and 330 nm over a temperature gradient from 35 to 95 °C, we observed no significant differences in the inflection temperatures (53.43 and 53.37 °C for the WT RBD and Y453F, respectively), suggesting that the variant has no critical effect on protein stability (Fig. 1B). We also determined the kinetics of the interaction with the ectodomain of human ACE-2 by biolayer interferometry (Fig. 1, C and D). The Y453F variant bound with a 4-fold higher affinity than the WT (3.85 nM vs 15.5 nM) and analyses of the K_a and K_{dis} revealed that it bound faster to ACE-2 (K_a 1.5×10^5 Ms vs 4×10^5 Ms) and remained bound for longer (7×10^{-4} s $^{-1}$ vs 6×10^{-3} s $^{-1}$).

Determination of the inhibition capacity of COVID-19 convalescent patients against the Y453F variant

To clarify whether the tyrosine to phenylalanine substitution in the surface of the RBD affects not only its functionality but also recognition by the immune system, we determined the inhibition potency of sera from qPCR-confirmed COVID-19

convalescent individuals ($n = 141$) using a previously described ACE-2/RBD antibody inhibition assay (19). We observed no significant difference between the inhibition of the two variants (Fig. 2A) and a tight linear relationship ($R^2 = 0.9430$) with a highly significant correlation ($\rho = 0.9711$, $p < 0.0001$) of the serum antibody inhibition capacity to both RBD variants (Fig. 2B).

Determination of the vaccine response in a preclinical animal model

Next, we evaluated the inhibition potency of polyclonal sera and mouse mAbs isolated from mice immunized with WT RBD or prefusion-stabilized spike protein as a preclinical vaccine model (described elsewhere (19)) (Fig. 3). Sera from RBD immunized mice inhibited the WT and Y453F RBD binding to ACE-2 with an IC_{50} of 28,369 and 26,579, respectively, several fold more effectively than sera from spike immunized mice (IC_{50} of 7,075 and 6,363, respectively) (Fig. 3A). More importantly, and regardless of the immunization strategy, the mouse sera did not show differences in the inhibition potency of the two RBD variants.

Finally, we compared the inhibition of high-affinity mAbs ($n = 18$) derived from immunized mice (Fig. 3B). Linear regression and Spearman rank correlation analyses of the IC_{50}

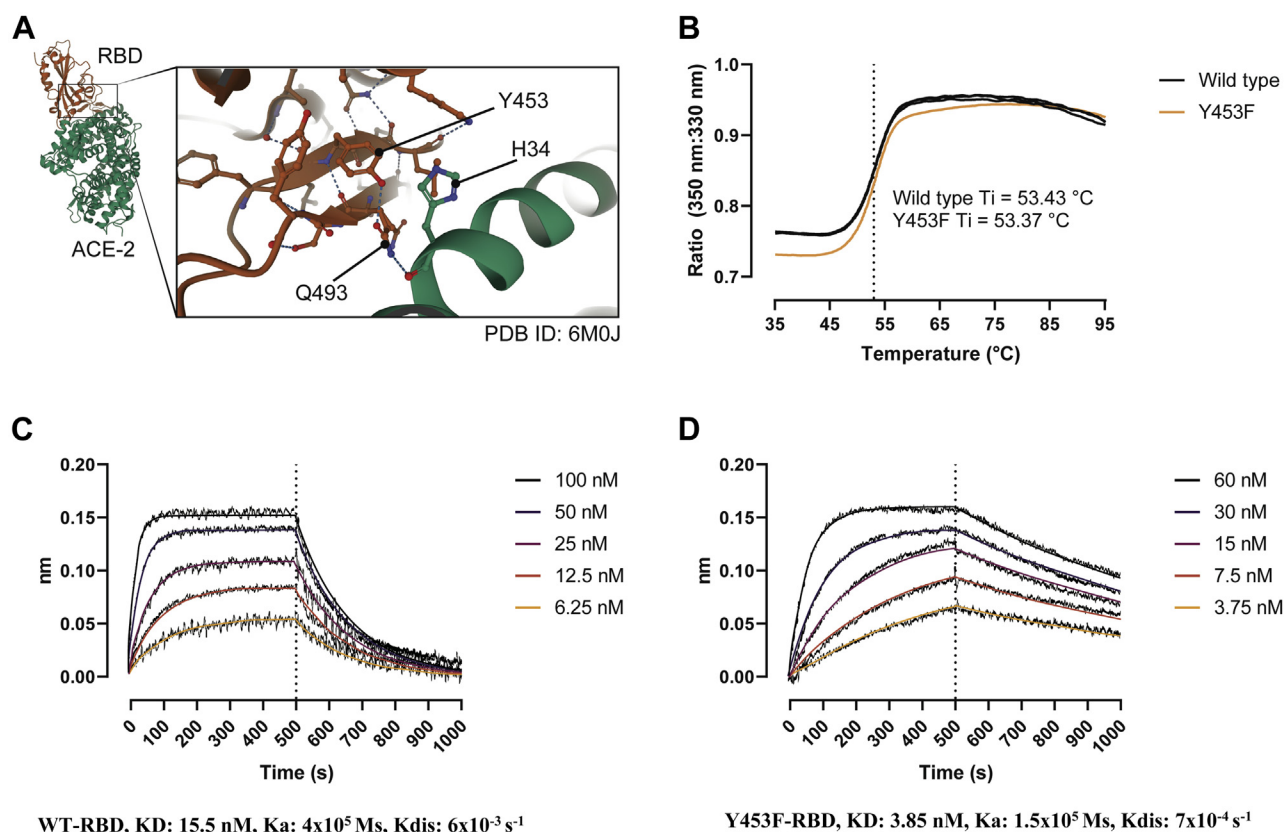


Figure 1. Biophysical characterization of WT and Y453F RBD. A, details of the binding interface of SARS-COV-2 RBD (orange) and the human ACE-2 receptor (green). The residue 453 maps to the receptor-binding motif within the RBD (residue 438–506) and directly engages the N-terminal helix of the peptidase domain of ACE-2 (30). Dashed lines represent noncovalent interactions. Created with PDB Molstar (<https://molstar.org/>). B, thermal denaturation curves of the WT and Y453F RBD. Data are represented as the 350:330 nm ratio of each replicate. C and D, WT (C) and Y453F (D) RBD binding response curves to ACE-2 determined by biolayer interferometry. ACE-2-Fc was immobilized onto anti-human IgG Fc capture sensors and dipped into serial dilutions of RBD (5-point 2-fold dilutions starting at 100 nM [WT] or 60 nM [Y453F]). T_i , inflection temperature; ACE-2, angiotensin-converting enzyme-2; RBD, receptor-binding domain.

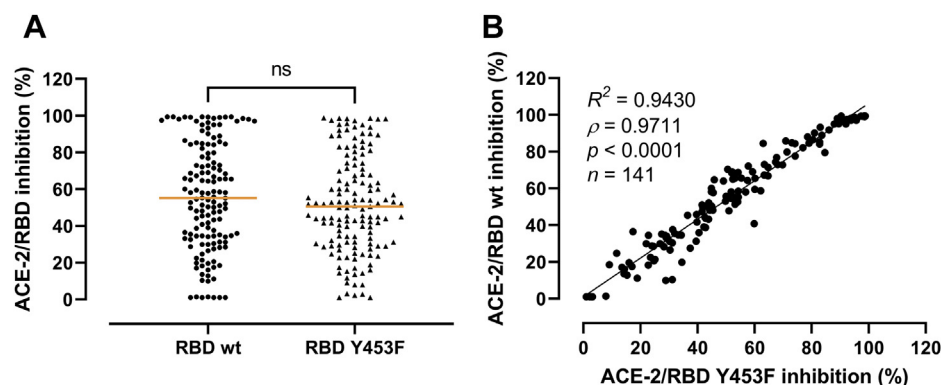


Figure 2. Inhibition potency of COVID-19 convalescent patient sera against the WT and Y453F RBD. A, distribution of the inhibition potency of COVID-19 patient sera against WT and Y453F RBD ($n = 141$), analyzed using the Mann-Whitney test. Orange lines represent the median. B, linear regression and Spearman rank correlation analyses of the data in panel A. The trend line represents a linear regression. Negative inhibition values were normalized to 0. Ns, not significant; RBD, receptor-binding domain.

values against WT and Y453F RBD revealed that the inhibition potencies against both variants correlated strongly ($R^2 = 0.9613$, $\rho = 0.8919$, $p < 0.0001$). The inhibition capacity of the individual mAbs was assessed separately.

Discussion

The emergence of nonsynonymous mutations in the SARS-CoV-2 spike gene has been reported since the beginning of 2020. The main part of these mutations has been identified within the European continent (>20), with fewer identifications on the Asian and American continents (20). The vast majority of these residue substitutions are located in the spike regions outside of the RBD with the D614G mutation being a common variant reported on all continents and which seems to be taking over likely because of selective advantages (21–25). Recently, three new genetic mutations inducing residue changes in the RBD have been reported in Europe, that is, N439K, Y453F, and N501Y. The N439K may make the virus more infectious because of an increased affinity toward ACE-2 and/or a reduced sensitivity to neutralizing antibodies (25–27). The N501Y mutant is a part of a novel strain, “Variant of Concern 202012/01”/B.1.1.7, that has accumulated 17 mutations—8 of them in the spike gene—and in some areas of

England may account for most of the new cases at the time of writing (18). The Y453F was first identified in Denmark in the summer of 2020 among farmed minks. The variant was coupled to the “cluster five” mutation (15) and arose a great international concern when it was reported to have been transmitted to humans. Millions of minks were culled and their pelts discarded, effectively shutting down a country-wide industry. However, a thorough functional characterization of the impact of the Y453F RBD variant on immunity and ACE-2 interaction has so far not been conducted.

When we challenged the RBD:ACE-2 interaction with COVID-19 convalescent sera from 141 qPCR-confirmed individuals that have been infected with the original SARS-CoV-2 variant, we found no reduction in the serum capacity to inhibit the binding of the Y453F variant to ACE-2. This conflicts with a preliminary report (“working paper”) that found that plasma samples from four convalescent individuals (out of a total of nine individuals) with low and intermediate neutralization titers had a reduced neutralization potency against the variant (15). The major difference in the study setups besides the number of included plasma samples is that the study from Lassauniere *et al.* (15) uses the bona fide plaque reduction neutralization test, where we have only addressed

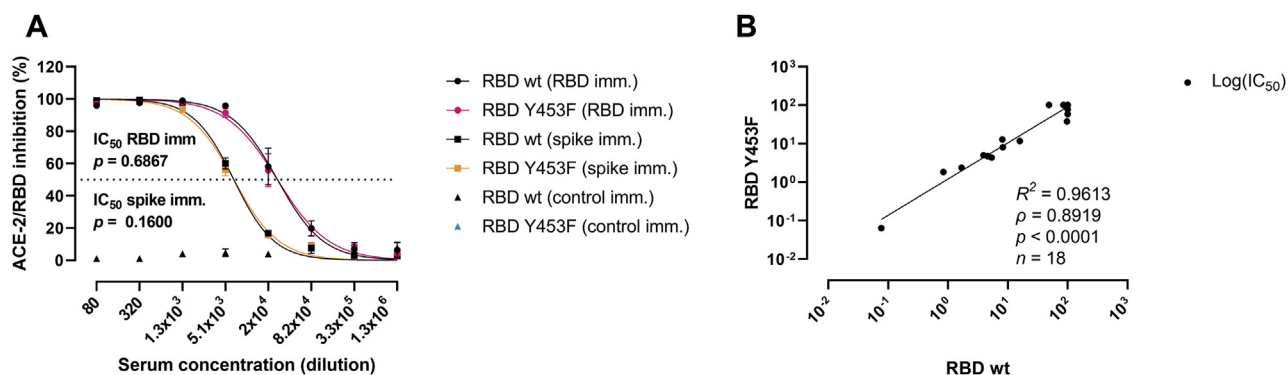


Figure 3. Inhibition potency of polyclonal sera and mAbs from mice immunized against SARS-CoV-2 WT spike or RBD. A, comparison of the best-fit IC_{50} of polyclonal sera from mice immunized with SARS-CoV-2 WT RBD (RBD imm.) or spike (spike imm.) against WT RBD (black symbols) and the Y453F variant (gray symbols). A SARS-CoV-2 nonrelated immunization (control imm.) was used as the control. Connecting lines represent the nonlinear fit. Data are presented as the mean \pm SEM. B, linear regression and Spearman rank correlation analyses of the inhibition potency ($\log[IC_{50}]$) of the WT and Y453F RBD using individual mAbs raised against WT RBD ($n = 10$) or WT spike ($n = 8$). RBD, receptor-binding domain.

the inhibition of the ACE-2/RBD interaction under less physiologically comparable conditions.

To further examine the possible inhibition differences between the two RBD variants, we used a traditional vaccine approach applying mice immunized with WT RBD or the full WT ectodomain spike and assessed the antibody titers and neutralization capacity of WT and Y453F RBD. In the vaccine models, we found no difference concerning the antibody-mediated ACE-2/RBD inhibition of the two variants, which was also the case when we challenged 18 different verified neutralizing mAbs raised against WT RBD or spike antigens.

The tyrosine at position 453 has been shown to be a critical residue engaged in direct interaction with the ACE-2 receptor *via* the tyr OH group (16). We therefore expected that there would be either a reduced or similar affinity with the substitution to a phenylalanine. However, to our surprise, we found a four-fold higher affinity of the 453F RBD binding to ACE-2 (KD 3.85 nM) compared with WT RBD. The precise reason for this remains to be established, but there are several other tyrosine residues in RBD that might be used in the ACE-2 interaction. The consequence of this affinity increase on the physiological avidity could even be more pronounced for the multimeric spike/ACE-2 interaction. However, since our findings are only indicative, caution should be taken when evaluating the transmission capacity of this SARS-CoV-2 variant.

Regardless, our results highlight two essential points regarding the developing clusters of spike variants: that immunity might not be dramatically challenged and that emphasis should also be placed on characterizing the transmission capacity and interaction properties of new emerging SARS-CoV-2 strains. This follows in the line of the new UK discovered N501Y mutant that within a short time gained transmission dominance in many areas including London, where by mid-December represented more than 60% of the cases (28). The functional properties of the N501Y mutant variant are not yet established.

Taken together, these results suggest that the molecular evolution of the SARS-CoV-2 virus has so far been taken in the direction of receptor affinity adaptation and optimization rather than toward an immune evasion strategy.

Experimental procedures

Production and biotinylation of recombinant proteins

The nucleotide sequence corresponding to the SARS-CoV-2 Y453F RBD variant with a C-terminal 10xHis-AviTag (SGSGHHHHHHHHHGGSLNDIFEAQKIEWHE) was synthesized and subcloned into a pcDNA3.4-TOPO expression vector by GeneArt (Thermo Fisher Scientific, MA). Recombinant Y453F RBD was produced by transiently transfecting Expi293 cells (Gibco, Thermo Fisher Scientific, MA) according to the manufacturer's recommendations. On day four after transfection, the supernatant was collected, and the protein was batch-purified by incubating 2 h at room temperature (RT) with HisPur Ni-NTA Resin (1 ml of sedimented resin/100 ml of supernatant) (Thermo Fisher Scientific) followed by wash and elution according to the manufacturer's instructions. The eluted

protein was subsequently applied to a HiLoad Superdex 16/600 200 pg size-exclusion chromatography column (Cytiva, MA) equilibrated in PBS. Purified RBD Y453F was buffer-exchanged and biotinylated on the C-terminal AviTag with a biotin ligase kit (Avidity, CO). The nucleotide sequence corresponding to the sequence of human ACE-2 ectodomain (aa. 17–740) with a CD33 signal peptide and a C-terminal human IgG1 was synthesized by Twist Bioscience (San Francisco, CA) and subcloned into a pTT5 expression vector. Recombinant ACE-2-Fc was produced by transiently transfecting Expi293 cells (Gibco, Thermo Fisher Scientific, MA) according to the manufacturer's recommendations. On day 5 after transfection, the supernatant was collected and the protein was affinity-purified on a 5-ml MabSelect SuRe column, followed by size-exclusion chromatography on a HiLoad Superdex 26/600 200 pg column (both Cytiva, MA) equilibrated in PBS. The production, purification, and biotinylation of the human ACE-2 receptor and SARS-CoV-2 WT RBD have been described elsewhere (19).

Thermal stability determination

The impact of the Y453F substitution on protein stability was analyzed on a Tycho NT.6 (NanoTemper technologies GmbH, Munich, Germany). RBD WT and Y453F were subjected in triplicates to a thermal ramp of 30 °C/min in PBS. Protein denaturation was monitored from the intrinsic fluorescence detected at 350 and 330 nm. Inflection temperatures representing a discrete unfolding event were calculated by the Tycho system from the 350:330 ratio.

RBD:ACE-2 affinity determination by biolayer interferometry

Binding kinetics experiments were performed on an Octet system (Octet RED384) (ForteBio, CA) in the 16-channel mode and loaded with anti-human Fc capture sensors (Pall Life Sciences, CA). Briefly (1), 13 µg/ml ACE-2-Fc was loaded on anti-human Fc capture tips (500 s) (2), base line (60 s) (3), association to 5-point 2-fold serial dilutions starting at 100 nM for WT RBD or 60 nM for Y453F RBD (500 s), and (4) the dissociation phase (500 s). Two specific reference sensors were assigned for each 16-channel column sensors, loaded with ACE-2-Fc and dipped into the running buffer during association and dissociation phases. The reference sensor sensorgrams were column-wise subtracted from sample sensorgrams. The running buffer was 20-mM Hepes, 150-mM NaCl, 5-mM CaCl₂, 0.1% BSA (IgG free), and 0.03% Tween-20, pH 7.4. Association and dissociation curves were globally fitted to a 1:1 binding model.

ACE-2/RBD antibody inhibition assay

The inhibition potency of COVID-19 convalescent sera, immunized mouse sera, and mAbs was determined *via* an *in house* ACE-2/RBD antibody inhibition ELISA-based method described elsewhere (19). Briefly, Nunc MaxiSorp microtiter plates (Invitrogen, Thermo Fisher Scientific) were coated with 1 µg/ml of ACE-2 overnight at 4 °C in PBS (10.1-mM Na₂HPO₄, 1.5-mM KH₂PO₄, 2.7-mM KCl, 137-mM NaCl). The next day, sera/mAbs were incubated for 1 h in

low-binding round-bottom plates (Thermo Fisher Scientific) with a solution of biotinylated WT or Y453F RBD (4 ng/ml) with HS-strep-HRP (1:16,000 dilution) in PBS with 0.05% Tween-20 (PBS-T) as follows: COVID-19 convalescent sera in a 10% dilution, immunized mouse sera in an 8-point 4-fold dilution starting at 1.25% dilution, and mAbs in a 6-point 4-fold dilution starting at 20 µg/ml. Afterward, the sera/mAbs:RBD:HS-Strep-HRP solution was transferred to ACE-2 plates and incubated for 15 min. The plates were developed with TMB One (Kem-En-Tec Diagnostics, Taastrup, Denmark) for 20 min and stopped with 0.3 M H₂SO₄. The absorbance was read at 450 nm. Between steps, the plates were washed thrice with PBS-T. Unless otherwise stated, all incubations were performed in an orbital shaker at RT.

Blood samples

A total of 141 serum samples from convalescent patients with a previously qPCR-confirmed SARS-CoV-2 infection were included in the study. The participants have been described elsewhere (29). A serum pool from healthy individuals collected before December 2019 was used as the negative control.

Ethics

The use of convalescent donor blood sample in this study has been approved by the Regional Ethical Committee of the Capital Region of Denmark with the approval ID: H-20028627. The human blood samples were obtained according to the Declaration of Helsinki.

The experimental animal procedures described in this study have been approved by the Danish Animal Experiments Inspectorate with the approval ID: 2019-15-0201-00090.

Statistics

Data analyses were performed with GraphPad Prism 9 (GraphPad Software, CA). The equation [inhibitor] vs normalized response with the variable slope was used to calculate the IC₅₀ values (from non-neutralizing serum samples and mAbs were normalized to 1 and 100, respectively). The relationship between the inhibition potency of sera and mAbs against the WT and Y453F RBD was estimated by the Mann-Whitney U test, linear regression analyses (reported as R²), and two-tailed Spearman rank correlation tests (reported as ρ and a significance value p). Best-fit IC₅₀ values of selected mAbs for WT and the Y453F RBD were compared with the extra-sum-of-squares F test. p values <0.05 were considered statistically significant.

Data availability

All data are contained within this article.

Acknowledgments—The authors would like to thank Jais Rose Bjelke, Frederik Kryh Öberg, and Per Franklin Nielsen from Novo Nordisk A/S for quality analysis of the recombinant proteins and Mss Camilla Xenia Holtermann Jahn, Sif Kaas Nielsen, and Jytte

Bryde Clausen, from the Laboratory of Molecular Medicine for their excellent technical assistance.

Author contributions—R. B.-O. and M.-O. S. conceived and designed the study; R. B.-O. and C. H. enabled recombinant protein production; R. B.-O., A. R., L. B. J., and M.-O. S. performed experiments; R. B.-O., L. B. J., and M.-O. S. analyzed the data; R. B.-O., P. G., and M.-O. S. wrote the paper with inputs from all co-authors. All authors approved the final version of the manuscript.

Funding and additional information—This work was financially supported by grants from the Carlsberg Foundation (CF20-0045 to M.-O. S., R. B.-O., and P. G.) and the Novo Nordisk Foundation (NFF205A0063505 and NNF20SA0064201 to M.-O. S., R. B.-O., and P. G.).

Conflict of interest—The authors declare that they have no conflicts of interest with the contents of this article.

Abbreviations—The abbreviations used are: ACE-2, angiotensin-converting enzyme 2; RBD, receptor-binding domain; SARS-CoV-2, Severe Acute Respiratory Syndrome Coronavirus 2.

References

- Shi, J., Wen, Z., Zhong, G., Yang, H., Wang, C., Huang, B., Liu, R., He, X., Shuai, L., Sun, Z., Zhao, Y., Liu, P., Liang, L., Cui, P., Wang, J., *et al.* (2020) Susceptibility of ferrets, cats, dogs, and other domesticated animals to SARS-coronavirus 2. *Science* **368**, 1016–1020
- Halfmann, P. J., Hatta, M., Chiba, S., Maemura, T., Fan, S., Takeda, M., Kinoshita, N., Hattori, S., Sakai-Tagawa, Y., Iwatsuki-Horimoto, K., Imai, M., and Kawaoka, Y. (2020) Transmission of SARS-CoV-2 in domestic cats. *N. Engl. J. Med.* **383**, 592–594
- Sia, S. F., Yan, L.-M., Chin, A. W. H., Fung, K., Choy, K.-T., Wong, A. Y. L., Kaewpreedee, P., Perera, R. A. P. M., Poon, L. L. M., Nicholls, J. M., Peiris, M., and Yen, H.-L. (2020) Pathogenesis and transmission of SARS-CoV-2 in golden hamsters. *Nature* **583**, 834–838
- Oreshkova, N., Molenaar, R. J., Vreman, S., Harders, F., Oude Munnink, B. B., Hakze-van der Honing, R. W., Gerhards, N., Tolsma, P., Bouwstra, R., Sikkema, R. S., Tacke, M. G., de Rooij, M. M., Weesendorp, E., Engelsma, M. Y., Bruschke, C. J., *et al.* (2020) SARS-CoV-2 infection in farmed minks, The Netherlands, April and May 2020. *Euro Surveill.* **25**, 2001005
- Sit, T. H. C., Brackman, C. J., Ip, S. M., Tam, K. W. S., Law, P. Y. T., To, E. M. W., Yu, V. Y. T., Sims, L. D., Tsang, D. N. C., Chu, D. K. W., Perera, R. A. P. M., Poon, L. L. M., and Peiris, M. (2020) Infection of dogs with SARS-CoV-2. *Nature* **586**, 776–778
- Patterson, E. I., Elia, G., Grassi, A., Giordano, A., Desario, C., Medardo, M., Smith, S. L., Anderson, E. R., Prince, T., Patterson, G. T., Lorusso, E., Lucente, M. S., Lanave, G., Lauzi, S., Bonfanti, U., *et al.* (2020) Evidence of exposure to SARS-CoV-2 in cats and dogs from households in Italy. *Nat. Commun.* **11**, 6231
- Newman, A., Smith, D., Ghai, R. R., Wallace, R. M., Torchetti, M. K., Loiacono, C., Murrell, L. S., Carpenter, A., Moroff, S., Rooney, J. A., and Barton Behravesh, C. (2020) First reported cases of SARS-CoV-2 infection in companion animals - New York, March-April 2020. *MMWR. Morb. Mortal. Wkly. Rep.* **69**, 710–713
- Yoo, H. S., and Yoo, D. (2020) COVID-19 and veterinarians for one health, zoonotic- and reverse-zoonotic transmissions. *J. Vet. Sci.* **21**, e51
- Molenaar, R. J., Vreman, S., Hakze-van der Honing, R. W., Zwart, R., de Rond, J., Weesendorp, E., Smit, L. A. M., Koopmans, M., Bouwstra, R., Stegeman, A., and van der Poel, W. H. M. (2020) Clinical and pathological findings in SARS-CoV-2 disease outbreaks in farmed mink (Neovison vison). *Vet. Pathol.* **57**, 653–657
- Oude Munnink, B. B., Sikkema, R. S., Nieuwenhuijse, D. F., Molenaar, R. J., Munger, E., Molenkamp, R., van der Spek, A., Tolsma, P., Rietveld, A.,

ACCELERATED COMMUNICATION: Y453F RBD shows a clear ACE-2 affinity increase

- Brouwer, M., Bouwmeester-Vincken, N., Harders, F., der Honing, R. H., Wegdam-Blans, M. C. A., Bouwstra, R. J., *et al.* (2021) Jumping back and forth: Anthropozoonotic and zoonotic transmission of SARS-CoV-2 on mink farms. *bioRxiv*. 1–35. <https://doi.org/10.1101/2020.09.01.277152>
- Walls, A. C., Park, Y.-J. J., Tortorici, M. A., Wall, A., McGuire, A. T., and Veelsler, D. (2020) Structure, function, and antigenicity of the SARS-CoV-2 spike Glycoprotein. *Cell* **181**, 281–292.e6
 - Hoffmann, M., Kleine-Weber, H., Schroeder, S., Krüger, N., Herrler, T., Erichsen, S., Schiergens, T. S., Herrler, G., Wu, N.-H. H., Nitsche, A., Müller, M. A., Drosten, C., and Pöhlmann, S. (2020) SARS-CoV-2 cell entry depends on ACE2 and TMPRSS2 and is blocked by a clinically proven protease inhibitor. *Cell* **181**, 271–280.e8
 - He, Y., Zhou, Y., Wu, H., Luo, B., Chen, J., Li, W., and Jiang, S. (2004) Identification of immunodominant sites on the spike protein of severe acute respiratory syndrome (SARS) coronavirus: Implication for developing SARS diagnostics and vaccines. *J. Immunol.* **173**, 4050–4057
 - Du, L., He, Y., Zhou, Y., Liu, S., Zheng, B. J., and Jiang, S. (2009) The spike protein of SARS-CoV - a target for vaccine and therapeutic development. *Nat. Rev. Microbiol.* **7**, 226–236
 - Lassaunière, R., Fonager, J., Rasmussen, M., Frische, A., Strandh, C. P., and Fomsgaard, V. A. (2020) *Working Paper on SARS-CoV-2 Spike Mutations Arising in Danish Mink, Their 1 Spread to Humans and Neutralization Data, Preliminary Report*. SSL, Copenhagen, Denmark: 1–7
 - Yan, R., Zhang, Y., Li, Y., Xia, L., Guo, Y., and Zhou, Q. (2021) Structural basis for the recognition of SARS-CoV-2 by full-length human ACE2. *Science* **367**, 1444–1448
 - Li, F., Li, W., Farzan, M., and Harrison, S. C. (2021) Structure of SARS coronavirus spike receptor-binding domain complexed with receptor. *Science* **309**, 1864–1868
 - Davies, N. G., Barnard, R. C., Jarvis, C. I., Kucharski, A. J., Munday, J., Pearson, C. A. B., Russell, T. W., Tully, D. C., Abbott, S., Gimma, A., Waites, W., Wong, K. L. M., van Zandvoort, K., Eggo, R. M., Funk, S., *et al.* (2021) Estimated transmissibility and impact of SARS-CoV-2 lineage B.1.1.7 in England. *medRxiv*. 1–80. <https://doi.org/10.1101/2020.12.24.20248822>
 - Bayarri-Olmos, R., Idorn, M., Rosbjerg, A., Pérez-Alós, L., Hansen, C., Johsen, L., Helgstrand, C., Öberg, F. K., Søgaard, M., Paludan, S., Bak-Thomsen, T., Jardine, J., Skjoedt, M.-O., and Garred, P. (2021) Vaccine monitoring shows that focused immunization with SARS-CoV-2 receptor-binding domain provides a better neutralizing antibody response than full-length spike protein. *Res. Sq.* 1–24. <https://doi.org/10.21203/rs.3.rs-134388/v1>
 - Mishra, D., Suri, G. S., Kaur, G., and Tiwari, M. (2021) Comparative insight into the genomic landscape of SARS-CoV-2 and identification of mutations associated with the origin of infection and diversity. *J. Med. Virol* **93**, 2406–2419
 - Zhang, L., Jackson, C. B., Mou, H., Ojha, A., Peng, H., Quinlan, B. D., Rangarajan, E. S., Pan, A., Vanderheiden, A., Suthar, M. S., Li, W., Izard, T., Rader, C., Farzan, M., and Choe, H. (2020) SARS-CoV-2 spike-protein D614G mutation increases virion spike density and infectivity. *Nat. Commun.* **11**, 6013
 - Yurkovetskiy, L., Wang, X., Pascal, K. E., Tomkins-Tinch, C., Nyalile, T. P., Wang, Y., Baum, A., Diehl, W. E., Dauphin, A., Carbone, C., Veinotte, K., Egri, S. B., Schaffner, S. F., Lemieux, J. E., Munro, J. B., *et al.* (2020) Structural and functional analysis of the D614G SARS-CoV-2 spike protein variant. *Cell* **183**, 739–751.e8
 - Korber, B., Fischer, W. M., Gnanakaran, S., Yoon, H., Theiler, J., Abfalterer, W., Hengartner, N., Giorgi, E. E., Bhattacharya, T., Foley, B., Hastie, K. M., Parker, M. D., Partridge, D. G., Evans, C. M., Freeman, T. M., *et al.* (2020) Tracking changes in SARS-CoV-2 spike: Evidence that D614G increases infectivity of the COVID-19 virus. *Cell* **182**, 812–827.e19
 - Plante, J. A., Liu, Y., Liu, J., Xia, H., Johnson, B. A., Lokugamage, K. G., Zhang, X., Muruato, A. E., Zou, J., Fontes-Garfias, C. R., Mirchandani, D., Scharton, D., Bilello, J. P., Ku, Z., An, Z., *et al.* (2021) Spike mutation D614G alters SARS-CoV-2 fitness. *Nature* **592**, 116–121. <https://doi.org/10.1038/s41586-020-2895-3>
 - Li, Q., Wu, J., Nie, J., Zhang, L., Hao, H., Liu, S., Zhao, C., Zhang, Q., Liu, H., Nie, L., Qin, H., Wang, M., Lu, Q., Li, X., Sun, Q., *et al.* (2020) The impact of mutations in SARS-CoV-2 spike on viral infectivity and antigenicity. *Cell* **182**, 1284–1294.e9
 - Zhou, W., Xu, C., Wang, P., Luo, M., Xu, Z., Cheng, R., Jin, X., Guo, Y., Xue, G., Juan, L., Nie, H., and Jiang, Q. (2020) N439K variant in spike protein may alter the infection efficiency and antigenicity of SARS-CoV-2 based on molecular dynamics simulation. *bioRxiv*. 1–18. <https://doi.org/10.1101/2020.11.21.392407>
 - Thomson, E. C., Rosen, L. E., Shepherd, J. G., Spreafico, R., da Silva Filipe, A., Wojcechowskyj, J. A., Davis, C., Piccoli, L., Pascall, D. J., Dillen, J., Lytras, S., Czudnochowski, N., Shah, R., Meury, M., Jesudason, N., *et al.* (2020) The circulating SARS-CoV-2 spike variant N439K maintains fitness while evading antibody-mediated immunity. *bioRxiv*. 1–31. <https://doi.org/10.1101/2020.11.04.355842>
 - Kupferschmidt, K. (2020) Mutant coronavirus in the United Kingdom sets off alarms, but its importance remains unclear. *Science (80-)*. <https://doi.org/10.1126/science.abg2626>
 - Hansen, C. B., Jarlhelt, I., Pérez-Alós, L., Hummelshøj Landsy, L., Loftager, M., Rosbjerg, A., Helgstrand, C., Bjelke, J. R., Egebjerg, T., Jardine, J. G., Sværke Jørgensen, C., Iversen, K., Bayarri-Olmos, R., Garred, P., and Skjoedt, M.-O. (2021) SARS-CoV-2 antibody responses are correlated to disease severity in COVID-19 convalescent individuals. *J. Immunol.* **206**, 109–117
 - Lan, J., Ge, J., Yu, J., Shan, S., Zhou, H., Fan, S., Zhang, Q., Shi, X., Wang, Q., Zhang, L., and Wang, X. (2020) Structure of the SARS-CoV-2 spike receptor-binding domain bound to the ACE2 receptor. *Nature* **581**, 215–220